

Copyright 2010, ABRACO

Trabalho apresentado durante o INTERCORR 2010, em Fortaleza/CE no mês de maio de 2010.

As informações e opiniões contidas neste trabalho são de exclusiva responsabilidade do(s) autor(es).

Optimization of rare earth additions to increase high temperature oxidation resistance of chromia and alumina forming alloys

Stela M. Fernandes¹, Olandir V. Correa², Lalgudi V.Ramanathan³

Abstract

Alloys for use at high temperatures often rely on the formation of protective layers of chromia or alumina. The use of reactive elements, mainly rare earths (RE) to improve high temperature oxidation resistance of chromia and alumina forming alloys is well known. The improvements in oxidation resistance are in the form of reduced oxidation rates and increased oxide scale adhesion. The RE can be added as alloying element or oxide additions (to form a dispersion) or applied as a coating to the alloy surface. Early studies carried out in IPEN indicated that the oxides of La, Pr and Nd were considerably more affective in decreasing oxidation rates compared to the traditional Ce and Y. Increasing demand in recent years for even higher oxidation resistant chromia and alumina forming alloys lead to attempts at optimizing RE additions. This optimization was done in the form of simultaneous addition of two different RE oxides. This paper presents the influence of surface additions of nanocrystalline oxides CeO₂, CeO₂ + La₂O₃ and CeO₂ + Pr₂O₃ on the isothermal oxidation behavior of Fe20Cr and Fe20Cr5Al alloys at 1000° C. The oxidation resistance of the Fe20Cr alloy coated with a mixture of Ce and La oxides was higher than that of the same alloy coated with either oxide and the latter, significantly more resistant than the uncoated alloy.

Key words: Iron-chromium alloy, iron-chromium-aluminum alloy, oxidation, rare earth oxide.

Introdução

Iron, nickel or cobalt based alloys are alloyed with chromium, aluminum or silicon to establish more protective oxides (scales) of chromia, alumina or silica respectively. Protective oxide scales should be non-volatile, stoichiometric, stress free at operating temperatures, adherent, and defect free. In practice, it is almost impossible to form such scales. Reactive elements, especially rare earths (RE) have been used to improve high temperature oxidation resistance of chromium dioxide and alumina forming alloys. The improvements are in the form of reduced oxidation rates and increased scale adhesion. (1, 2) The RE can be added to the alloy as elements or as oxide to form dispersions. It can also be introduced into the surface by ion implantation or applied as an oxide coating to the surface

¹ Ph.D. – Pesquisadora, IPEN, São Paulo. Brasil

² Técnico - IPEN, São Paulo. Brasil

³ Ph.D. – Pesquisador, Gerente Geral, IPEN, São Paulo. Brasil

of the alloy.(2-4) A variety of precursors have been used to obtain RE oxide coatings on metallic surfaces. The use of sols, followed by its transformation to gel is referred to as the sol-gel technique and it produces oxide particles in the range 2 nm to 1 μm . (5)

The sol can be applied to a metallic substrate by a suitable technique, such as dipping, spin coating or electrophoresis. Compared to adding RE to the alloy, RE oxide coatings do not affect adversely the mechanical properties of the alloy. The oxide coatings can be also used on metallic components in service and exposed to high temperature oxidizing environments. The marked influence of surface deposited RE oxides on the isothermal and cyclic oxidation behavior has been observed and reported. (6,7) Nevertheless, increasing demand in recent years for even higher oxidation resistant chromia and alumina forming alloys has lead to attempts at optimizing RE additions. In this investigation, this optimization was done in the form of simultaneous addition of two different RE oxides. This paper presents the effect of surface addition of nanocrystalline oxide gels of cerium oxide and lanthanum oxide, both as single or as mixed oxides on the oxidation behavior of Fe20Cr and Fe20Cr5Al alloys. The mechanism by which these REs improved overall oxidation resistance of the alloys is also discussed.

Methods and materials

In preliminary investigations Sols of La_2O_3 , CeO_2 , Pr_2O_3 , Nd_2O_3 , Sm_2O_3 , Gd_2O_3 , Dy_2O_3 , Y_2O_3 , Er_2O_3 , and Yb_2O_3 , were prepared as aqueous dispersions of the respective rare earth oxides with nitric acid, and a non-ionic surfactant. The solution was heated to 80°C under constant agitation for an hour and the sol formed as sediment. Fe-20Cr alloy specimens $1.0 \times 1.0 \times 0.5 \text{ cm}$ were ground to 400 mesh, rinsed and dried. The RE oxide sol was sprayed on the specimen to form a coat. The specimens were then heated to 150°C to form a $10 \mu\text{m}$ thick surface layer of RE oxide gel. The morphology of these oxides, the size of the crystallites of these oxides, the extent to which these oxides covered the substrates and the overall influence of these oxides on the isothermal and cyclic oxidation behavior of the substrate alloy was studied. In a subsequent study, sols of CeO_2 , La_2O_3 , Pr_2O_3 , $\text{CeO}_2 + \text{La}_2\text{O}_3$ and $\text{CeO}_2 + \text{Pr}_2\text{O}_3$ were prepared to coat Fe20Cr and Fe20Cr5Al alloy specimens (approximate dimensions $2 \times 2 \times 3 \text{ mm}$) and form the respective gels. These specimens were isothermally oxidized at 1000°C for about 400 minutes in a thermal balance. The weight gain per unit area versus time curves weas plotted. The specimens surfaces were then examined in a scanning electron microscope (SEM) coupled to an energy dispersive spectroscopy (EDS) system.

Results and discussion

Scanning electron micrographs of the different RE oxide gels are shown in figure 1. Marked differences in the morphology of the oxides can be seen. Table I summarizes the morphological characteristics of the oxides. Table II shows the cyclic oxidation behavior of the Fe20Cr alloy coated with the different RE oxides. Comparison of data in tables I and II indicates a correlation between the morphology of the RE oxide and the cyclic oxidation resistance of the specimen coated with that RE oxide. Specimens coated RE oxides with cube, rod or needle-like morphology withstood a higher number of oxidation cycles compared to those coated with RE oxides with platelet or cluster morphology.

Figures 2a and 2b show the micrographs of the alloy surface covered with La_2O_3 and Yb_2O_3 . Marked differences are evident in the extent to which the surfaces are covered by the two

oxides. The two oxides, La_2O_3 and Yb_2O_3 , have very high and low coverage. The area fractions, or coverage, of these two oxides and the other oxides were determined from image analysis measurements. The coverage of the different RE oxide is summarized in table III. The cyclic oxidation resistance of the alloy coated with the different RE oxides is also shown in table III, to help correlate the two parameters. This table clearly indicates a correspondence between the extent of coverage and the cyclic oxidation resistance. The exceptions are cerium and gadolinium oxides. The influence of the former can be attributed to its valence. Cerium oxide has the formula CeO_2 where as the other RE oxides have the general formula RE_2O_3 .

On the basis of the following observations: low cost combined with moderate influence of CeO_2 on oxidation resistance of FeCr alloy; higher influence of La_2O_3 and Pr_2O_3 on oxidation resistance of the same alloy; the role of rare earth ion radius, the influence of rare earth oxide morphology; varying coverages of the different RE oxides, the second set of investigations were undertaken to attempt optimization of the influence of RE oxides. The first step was therefore to evaluate the effect of simultaneous addition of RE oxides.

The isothermal oxidation curves of uncoated and RE oxide coated specimens is shown in figures 1 and 2. The weight gain of the uncoated and RE oxide coated Fe20Cr and Fe20Cr5Al specimens during oxidation is due to formation of Cr_2O_3 and Al_2O_3 respectively on the specimen surfaces. (6,7)

Figure 3 shows the oxidation curves of uncoated Fe20Cr, CeO_2 coated Fe20Cr, La_2O_3 coated Fe20Cr, $\text{CeO}_2 + \text{La}_2\text{O}_3$ coated Fe20Cr and $\text{CeO}_2 + \text{La}_2\text{O}_3$ coated Fe20Cr5Al specimens. The chromium dioxide layer on both the uncoated and RE oxide coated Fe20Cr specimens as well as the alumina layer on the Fe20Cr5Al specimens did not spall. All the specimens revealed parabolic oxidation behavior. The effect of rare earth oxide addition to the surface of the FeCr alloy was clearly evident upon comparison of the curves of Fe20Cr and the other RE oxide covered Fe20Cr specimens. Substitution of CeO_2 with La_2O_3 showed a slight improvement in oxidation behavior. However, when the two oxides CeO_2 and La_2O_3 were jointly present on the surface, the improvement in oxidation resistance was marked. The curve of the Fe20Cr5Al specimen indicated even higher oxidation resistance. This could be attributed to the joint effect of the low oxidation rate of alumina formers and the effect of the rare earth ion on alumina formation. Work is ongoing to separate these two effects. Figure 4 shows the curves of uncoated Fe20Cr, CeO_2 coated Fe20Cr, Pr_2O_3 coated Fe20Cr and $\text{CeO}_2 + \text{Pr}_2\text{O}_3$ coated Fe20Cr specimens. Observations similar to those made earlier about the influence of La_2O_3 additions can be also made for Pr_2O_3 additions.

4 General discussions

The morphology of the different RE oxide gels revealed marked differences. (3, 7) Correlations between the morphology of the RE oxide and the COR of coated Fe-20Cr alloy have been reported. (7) Specimens coated with RE oxides with cube, rod or needle-like morphology withstood a higher number of oxidation cycles compared to those coated with RE oxides with platelet or cluster morphology. Coverage, or the extent to which the Fe-20Cr surface was covered by the different RE oxides also varied and correspondence between coverage and COR has been reported. (7)

A mixed Ce and La oxide is considered to have higher coverage.

In previous studies it was shown that in the presence of an RE oxide coating the chromium dioxide layer formed is thinner than that on surfaces without a RE oxide coating and this varied with RE oxide.

Marked variations in the extent to which different RE oxides affect oxidation rate of specially chromia forming alloys was attributed to RE ion radius. That is biggest the radius, greater was the influence of the RE in mitigating chromia scale growth. [dd] Similar effect on alumina growth rate, but to a lower extent has been reported. [ff]

The RE oxide crystallite size also has an effect on chromia and alumina growth rates.

In the initial or transient stage of oxidation, metastable oxides of base metals such as iron oxide, form on the alloy surface. The effects of RE on scale growth are not evident at this stage. Some of the REs exercise greater influence than others. (7) In the absence of RE in the alloy or on the surface, the new oxide scale grows at the oxide /oxygen interface and in the presence of RE it grows at the metal/oxide interface.

In the case where REs are added to the alloy, the reactive elements in the alloy diffuse into the scale due to the oxygen potential gradient which extends from the gas interface into the substrate. The RE diffuses through the oxide to the gas interface. Proof of this was shown after prolonged oxidations.(8) En-route to the gas interface the RE ions first segregate to the metal-scale interface and then these RE ions follow the fastest path to the gas interface, which are the scale grain boundaries.(9-15) This is shown schematically in Figure 2. The RE oxides applied as coatings to the alloy surface is incorporated in the growing scale.(6) Their ions segregate to the scale grain boundaries.

There is evidence that RE-base metal mixed oxides form at oxide scale grain boundaries, which depletes the amount of RE ion available at the scale boundaries to block outward base metal cation diffusion to the oxide/oxygen interface.

It is believed that in the presence of two different RE oxides on the alloy surface the two RE oxides get incorporated into the scale and segregate to the scale grain boundaries. Spinel formation if energetically favorable at a specific place would cause depletion locally of just one of the two RE oxide ions, leaving behind the other RE ion to play the role of hindering Cr or Al ion diffusion to the gas interface.

When the RE ion concentration at the grain boundaries reaches a critical amount it results in the two effects that have been observed in this study.

The first effect is inhibition of normal outward short-circuit transport of alloy cations along the scale grain boundaries due to the slower diffusion of the large RE ions. It is also probable that RE with higher ionic radius diffuse slower along the grain boundaries compared with the RE ion with a smaller radius. Hence, bigger the RE ion, higher is the inhibition of alloy cation transport.(8, 14)

The second effect is reduction in scale grain growth and this is due a solute-drag effect of the RE ions on the scale grain boundaries.(16) This results in a smaller average grain size in α -Cr₂O₃ scales and higher scale plasticity.(17) In general, spalling occurs when scale thickness, reflected as mass gains per unit area in oxidation measurements is above a certain

value. This was found to be 1.25-1.5 mg.cm⁻² for chromia growth in this study. This indicated that the time at temperature to reach a specific chromia layer thickness varied with the nature of RE.

What about alumina. ??

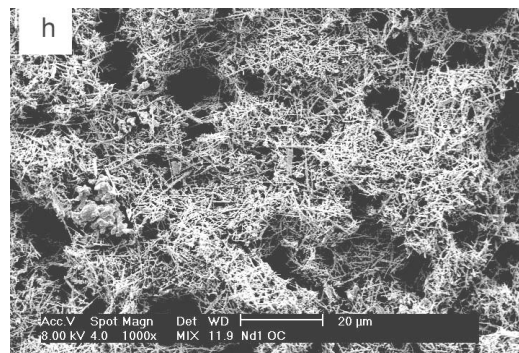
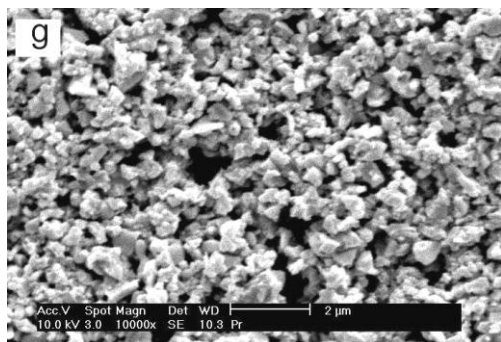
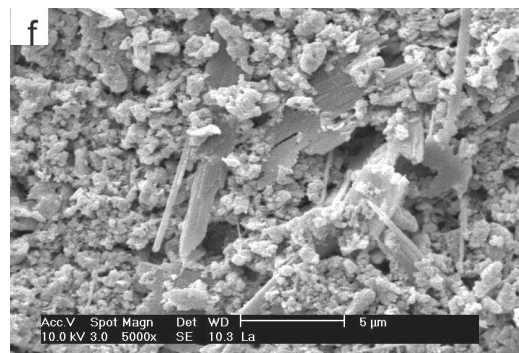
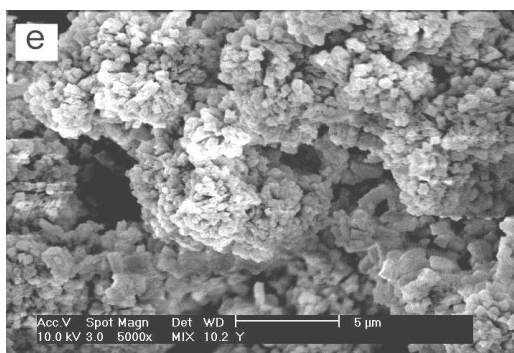
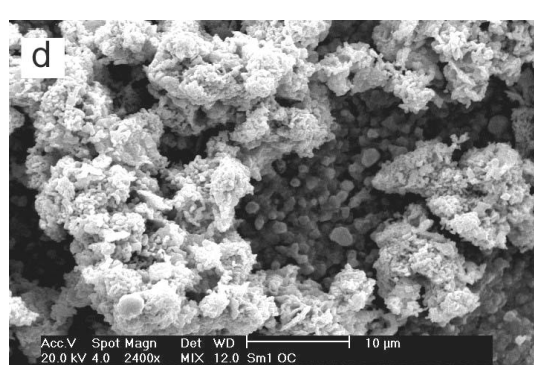
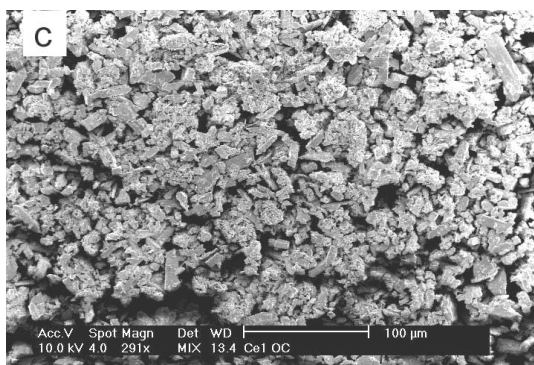
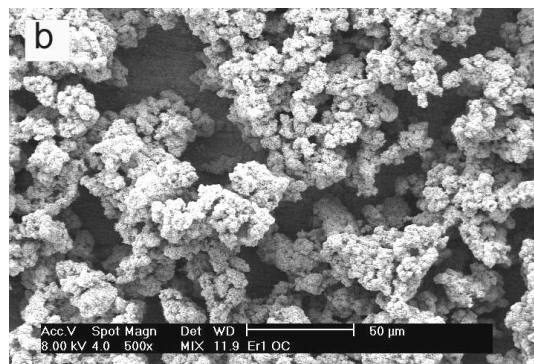
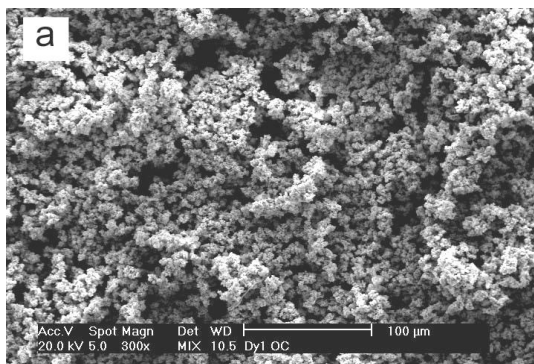
5 Conclusions

1. The oxidation resistance of RE oxide coated Fe20Cr alloy was significantly higher than that of the uncoated alloy.
2. The chromium dioxide layer thickness on the RE oxide coated Fe-20Cr alloy varied with the RE oxide.
3. The OR of Fe-20Cr coated with La₂O₃ was significantly higher than that of the same alloy coated with CeO₂.
4. The OR of Fe-20Cr coated with CeO₂ and La₂O₃ was even higher than that of the same alloy coated with either REO.
5. The OR of the Al containing alloy coated simultaneously with the two oxides was even higher.
6. The marked increase in the OR of the two alloys coated with the two REO compared to that coated with either oxide has been attributed to optimization in REO grain size and shape, resulting in increased surface coverage and also to optimization in the chemical potentials of two REO with ionic radii very close to one another.

References

1. STOTT, F.H. Influence of alloy additions on oxidation. **Materials Science and Technology**, v.5, p.734-740, 1989.
2. STRINGER, J. The reactive elements effect in high temperature corrosion. **Materials Science and Engineering**, v. A120, p.129-137, 1989.
3. HOU, P.Y.; STRINGER, J. The effect of surface applied reactive metal oxide on the high temperature oxidation of alloys. **Materials Science and Engineering**. v. 87, p. 295-302, 1987.
4. RAMANATHAN, L.V. Role of rare earth elements on high temperature oxidation behavior of Fe-Cr, Ni-Cr and Ni-Cr-Al alloys. **Corrosion Science**, v 35 (5-8), p. 871-878, 1993.
5. BENNET, M.J. New coatings for high temperature materials protection. **Journal of Vacuum Science and Technology**, v. B2 (4), p.800-805, 1984.
6. FERNANDES, S.M.C.; RAMANATHAN, L.V. Influence of rare earth oxide coatings on oxidation behavior of Fe-20Cr alloys. **Surface Engineering**. v.16 (4) p. 327-332, 2000.
7. FERNANDES, S.M.C.; RAMANATHAN, L.V. Effect of surface deposited rare earth oxide gel characteristics on cyclic oxidation behavior of Fe20-Cr alloys. **Materials Research**, v. 9, 2, p.199-203, 2006.
8. PINT, B. Experimental observations in support of the dynamic-segregation theory to explain the reactive-element effect. **Oxidation of Metals**, v. 45, p. 1, 1996.

9. COTELL, C.M.; YUREK, G.J.; HUSSEY, R.J.; MITCHELL, D.F.; GRAHAM, M.J. The influence of grain boundary segregation of yttrium in chromium dioxide on the oxidation of chromium metal. **Oxidation of Metals**, v. 34, p.173-200, p. 201-216, 1990.
10. VERSACI, R.A.; CLEMENS, D.; QUADAKKERS, W.J.; HUSSEY, R. Distribution and transport of yttrium in alumina scales on iron-base ODS alloys. **Solid State Ionics**, v. 59, p.235-242, 1993.
11. PINT, B.; MARTIN, J.R.; HOBBS, L.W. ^{18}O / SIMS Characterization of the growth mechanism of doped and undoped $\alpha\text{-Al}_2\text{O}_3$. **Oxidation of Metals**, v. 39, p.167, 1993.
12. PINT, B.; HOBBS, L.W. The formation of $\alpha\text{-Al}_2\text{O}_3$ scales at 1500° C, **Oxidation of Metals**, v. 41, p.203-233, 1994.
13. PINT, B.; HOBBS, L.W. Limitations on the use of ion implantation for the study of the reactive element effect in $\beta\text{-NiAl}$, **Journal of Electrochemical Society**, v. 141, p.2443, 1994.
14. PINT, B.; GARRATT-REED, A.J.; HOBBS, L.W. The reactive element effect in ODS FeCrAl alloys, **Materials at High temperatures**, v. 13, p.3-16, 1995,
15. PAPAIACOVOU, P.; HUSSEY, R.J. The effect of CeO_2 coatings on the oxidation behavior of Fe-20Cr alloys in O_2 at 1173K. **Corrosion Science**, v. 30(4/5), p.451-460, 1990.
16. KINGERY, W.D.; BOWEN, H.K.; UHLMANN, D.R. Introduction to ceramics, Wiley, New York, 1976.
17. RAMANARAYANAN, T.A.; RAGHAVAN, M.; PETKOVIC-LUTON, R. The Characteristics of alumina scales formed on Fe-based yttria-dispersed alloys, **Journal of Electrochemical Society**, v.131, p.923, 1984.



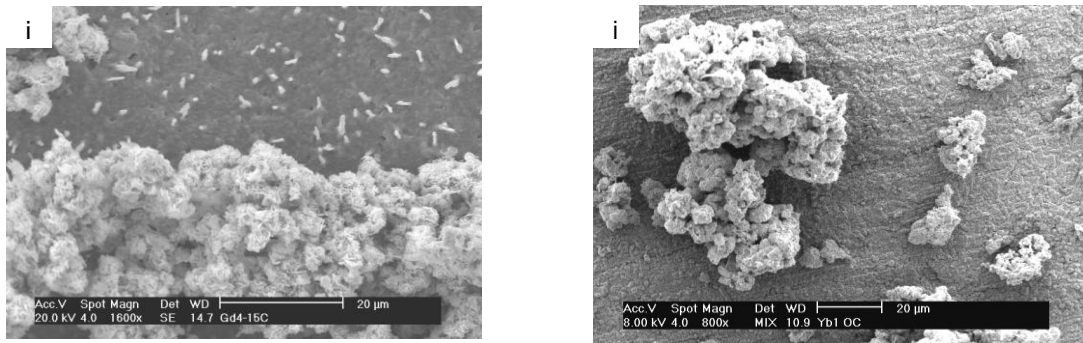


Figure 2: Scanning electron micrographs of different RE oxides. (a) Dy, (b) Er, (c) Ce, (d) Sm, (e) Y, (f) La, (g) Pr, (h) Nd, (i) Gd and (j) Yb.

Table I: Main morphological feature of the rare earth oxides

<i>Rare earth oxide</i>	<i>Main morphological feature</i>
Lanthanum	Cubes and rods
Cerium	Cubes
Praseodymium	Cuboids
Neodymium	Fine needles, acicular
Samarium	Clusters
Gadolinium	Interlocking clusters
Dysprosium	Tiny clusters
Yttrium	Platelets
Erbium	Open clusters
Ytterbium	Clusters and disperse platelets

Table I: Cyclic oxidation resistance of RE oxide coated Fe₂₀Cr alloy, expressed as the number of cycles of oxidation to spalling and the ratios of the RE ion radius to the radius of chromium ion.

Oxide of	Number of cycles at spall	R_{RE}/R_{Cr} ratio
Lanthanum	15+	1.64
Cerium	9	1.60
Praseodymium	15+	1.57
Neodymium	12	1.54
Samarium	12	1.50
Gadolinium	15+	1.46
Dysprosium	6	1.42
Yttrium	7	1.39
Erbium	7	1.37
Ytterbium	4	1.34

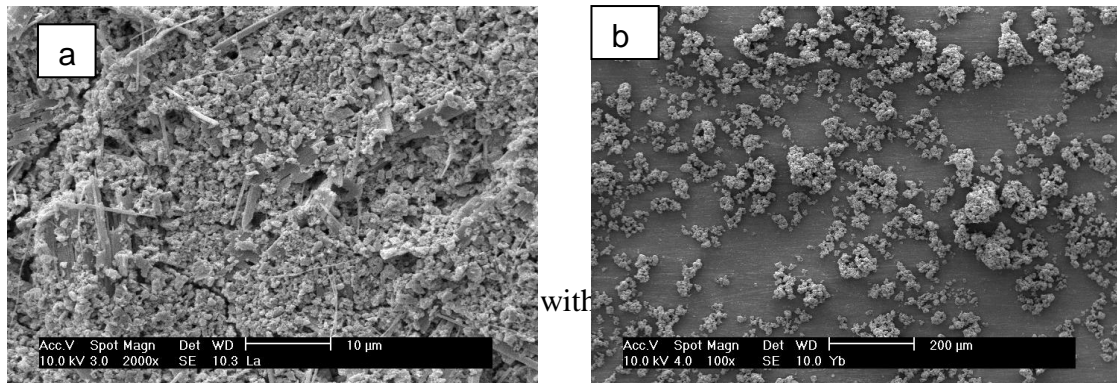


Table III: Correlation between coverage of RE oxide coat and cyclic oxidation resistance.

Rare earth oxide	Ranking of RE oxide coverage	Number of cycles to spall or cyclic oxidation resistance
Lanthanum	1	15
Cerium	6	9
Praseodymium	2	15
Neodymium	3	12
Samarium	4	12
Gadolinium	8	15
Dysprosium	5	6
Yttrium	7	7
Erbium	9	7
Ytterbium	10	4

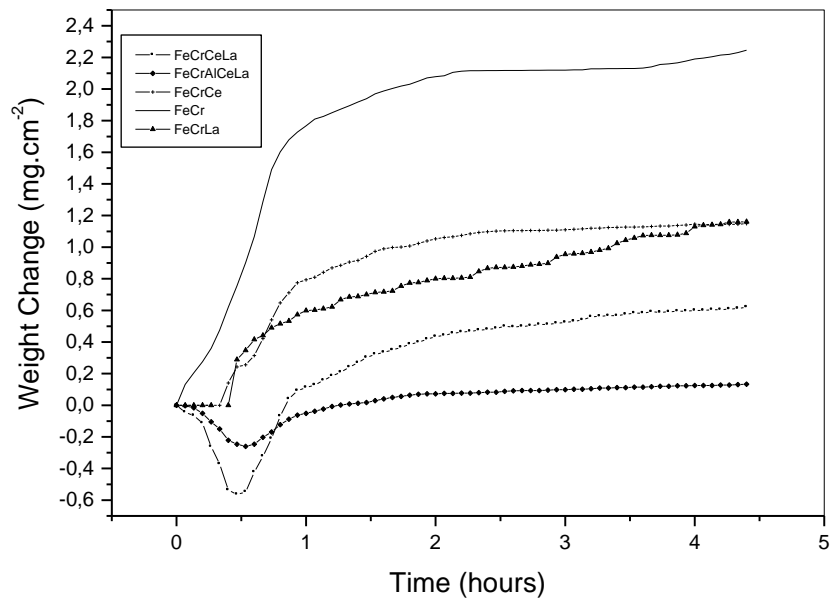


Figure 4. Isothermal oxidation curves of uncoated, CeO_2 coated, La_2O_3 coated and $\text{CeO}_2 + \text{La}_2\text{O}_3$ coated Fe20Cr as well as $\text{CeO}_2 + \text{La}_2\text{O}_3$ coated Fe20Cr5Al at 1000 °C.

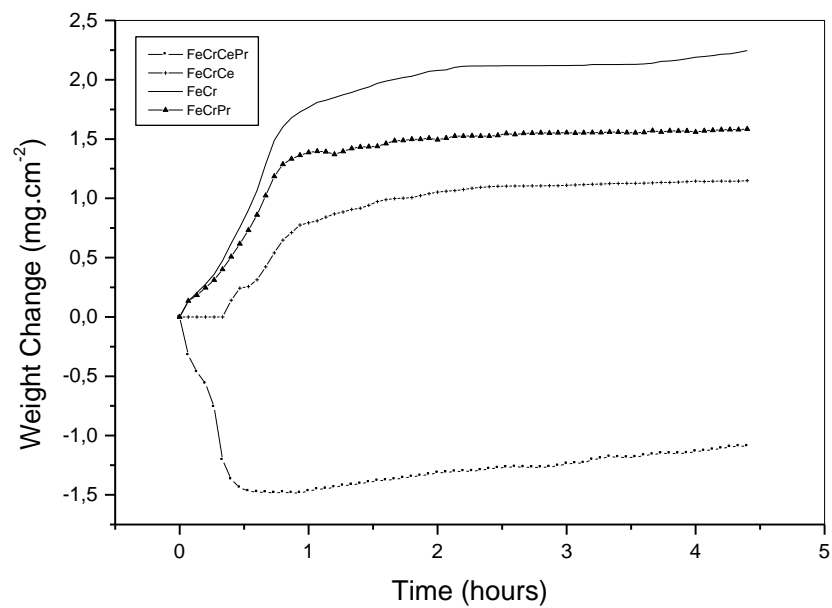


Figure 5. Isothermal oxidation curves of uncoated, CeO_2 coated, Pr_2O_3 coated and $\text{CeO}_2 + \text{Pr}_2\text{O}_3$ coated Fe20Cr at 1000 °C.